THE JOURNAL OF BIOLOGICAL CHEMISTRY VOL. 281, NO. 19, pp. 13324–13332, May 12, 2006

Crystal Structure of the Biglycan Dimer and Evidence That Dimerization Is Essential for Folding and Stability of Class I Small Leucine-rich Repeat Proteoglycans*

Received for publication, December 19, 2005, and in revised form, February 22, 2006 Published, JBC Papers in Press, March 17, 2006, DOI 10.1074/jbc.M513470200

Paul G. Scott[‡1], **Carole M. Dodd**[‡], **Ernst M. Bergmann**[‡§], **John K. Sheehan**[¶2], **and Paul N. Bishop**[¶3]

From the [‡]*Department of Biochemistry and the* [§]*Alberta Synchrotron Institute, Research Transition Facility, University of Alberta, Edmonton, Alberta T6G 2H7, Canada and the* [¶]*Wellcome Trust Centre for Cell-Matrix Research, Faculty of Life Sciences and Academic Unit of Eye & Vision Science, The Medical School, University of Manchester, Manchester M13 9PL, Great Britain*

Biglycan and decorin are two closely related proteoglycans whose protein cores contain leucine-rich repeats flanked by disulfides. We have previously shown that decorin is dimeric both in solution and in crystal structures. In this study we determined whether biglycan dimerizes and investigated the role of dimerization in the folding and stability of these proteoglycans. We used light scattering to show that biglycan is dimeric in solution and solved the crystal structure of the glycoprotein core of biglycan at 3.40-Å resolution. This structure reveals that biglycan dimerizes in the same way as decorin, *i.e.* by apposition of the concave inner surfaces of the leucine-rich repeat domains. We demonstrate that low concentrations of guanidinium chloride denature biglycan and decorin but that the denaturation is completely reversible following removal of the guanidinium chloride, as assessed by circular dichroism spectroscopy. Furthermore, the rate of refolding is dependent on protein concentration, demonstrating that it is not a unimolecular process. Upon heating, decorin shows a single structural transition at a T_m of 45–46 °C but refolds completely upon cooling to 25 °C. This property of decorin enabled us to show both by calorimetry and light scattering that dimer to monomer transition coincided with unfolding and monomer to dimer transition coincided with refolding; thus these processes are inextricably linked. We further conclude that folded monomeric biglycan or decorin cannot exist in solution. This implies novel interrelated functions for the parallel β sheet faces of these leucine-rich repeat proteoglycans, including dimerization and stabilization of protein folding.

The small leucine-rich repeat proteoglycans/proteins (SLRPs)[4] are a family of extracellular matrix molecules characterized by the presence of tandem leucine-rich repeats (LRRs) flanked by disulfides. Most members of the SLRP family can be divided into three subclasses with Class I containing decorin, biglycan, and asporin; Class II containing fibromodulin, lumican, keratocan, PRELP, and osteoadherin/osteomodulin; with Class III containing epiphycan/PG-Lb, mimecan/osteoglycin, and opticin (1). The archetypal SLRP is decorin, which is present in most connective tissues bound to the surfaces of collagen fibrils in a periodic array (2). Its functions are believed to include the regulation of the formation and/or organization of collagen fibrils (2, 3), inhibition of calcification of soft connective tissues (4), modulation of the activity of growth factors such as transforming growth factor-β (5), and other effects on cell proliferation and behavior (6, 7). Decorin contains 329 or 330 (8–10) amino acids and in most species has a single dermatan or chondroitin sulfate glycosaminoglycan (GAG) attached near the N terminus, at Ser-4 (11), and three *N*-linked oligosaccharides attached to the LRR domain (12). The protein core of biglycan contains 330 amino acids and shows 55% sequence identity to decorin. It carries two GAG chains near the N terminus and two *N*-linked oligosaccharides (13). Biglycan was first observed in extracts of mineralized bone (14) and is the most abundant small proteoglycan in articular cartilage (15) and in fibrocartilages such as the knee meniscus (16). A role in osteogenesis is indicated by the phenotype of the biglycan-null male mouse that develops severe osteoporosis (17). Immunohistochemistry showed biglycan to be predominantly located close to cell surfaces (18). It has been reported not to compete with decorin for binding to nascent collagen fibrils (19) or to bind less strongly (20).

The amino acid sequences of decorin and biglycan include 12 tandem LRRs averaging 24 residues long (21). LRRs are present in many intracellular, cell-surface, and extracellular proteins and consist of a strongly conserved core of 11 residues (L*XX*L*X*L*XX*N*X*I), flanked by more variable sequences (22). The LRR domains of the SLRPs are flanked by clusters of cysteines, four on the N-terminal side and two (usually) on the C-terminal side. These cysteines form disulfides that have been shown to be required for the biological activity of decorin (23) and fibromodulin (16), because reduction abolishes collagen binding.

We have previously shown that decorin and the Class III SLRP opticin form stable dimers in solution and that this dimerization is mediated through interactions between the LRR domains (24, 25). The decorin dimerization data were initially criticized on the grounds that the proteoglycan had been lyophilized during purification and that this could have caused nonspecific aggregation (26), but we subsequently showed that recombinant decorin that had neither been lyophilized nor exposed to denaturant was entirely dimeric (27). We also solved the crystal structures of both tissue-extracted and recombinant decorin,

* This work was supported in part by the Canadian Institutes for Health Research (Grant MOP 53175) and by the Wellcome Trust. X-ray diffraction data were collected at beamline 8.3.1 of the Advanced Light Source (ALS) at Lawrence Berkeley National Laboratory under an agreement with the Alberta Synchrotron Institute (ASI). The ALS is operated by the Department of Energy and supported by the National Institutes of Health. Beamline 8.3.1 was funded by the National Science Foundation, the University of California, and Henry Wheeler. The ASI synchrotron access program is supported by the Alberta Science and Research Authority, the Alberta Heritage Foundation for Medical Research, and the Alberta Ingenuity Fund. The costs of publication of this article were defrayed in part by the payment of page charges. This article must therefore be hereby marked "*advertisement*" in accordance with 18 U.S.C. Section 1734 solely to indicate this fact.

The atomic coordinates and structure factors (code 2FT3) have been deposited in the Protein Data Bank, Research Collaboratory for Structural Bioinformatics, Rutgers University, New Brunswick, NJ (http://www.rcsb.org/).

[1] To whom correspondence should be addressed: Dept. of Biochemistry, University of Alberta, 474 Medical Sciences Bldg., Edmonton, Alberta T6G 2H7, Canada. Tel.: 780-492-5755; Fax: 780-492-0886; E-mail: Paul.Scott@ualberta.ca.

[2] Present address: Cystic Fibrosis Center, University of North Carolina, Chapel Hill, NC 27599-7248.

[3] A Wellcome Trust Senior Research Fellow in Clinical Science.

[4] The abbreviations used are: SLRP, small leucine-rich repeat protein/proteoglycan; GAG, glycosaminoglycan; GdnHCl, guanidinium hydrochloride; LRR, leucine rich-repeat; TBS, Tris-buffered saline; Tris, Tris(hydroxymethyl)aminomethane; MALDI-TOF, matrix-assisted laser desorption ionization time-of-flight; r.m.s.d., root mean square deviation.

TABLE 1
Data collection statistics

Wavelength (Å)	1.0
Temperature (K)	90
Resolution range (outer shell) (Å)	22.86–3.40 (3.58–3.40)
No. of observations	
Measured	122,151
Unique	40,717
Completeness (%)	
Overall	96.5
Last shell	97.7
R_{sym}[a] (%)	35.5
Average $I/\sigma I$	3.4

[a] $R_{sym} = \Sigma_h\Sigma_i|I_i(h) - \langle I(h)\rangle|/\Sigma_h I(h)$, where $I_i(h)$ is the ith measurement of the h reflection and $\langle I(h)\rangle$ is the average value of the reflection intensity.

TABLE 2
Refinement statistics

Refinement	
Resolution range (outer shell) (Å)	22.86–3.40 (3.49–3.40)
R_{cryst}[a] (%)	25.9 (33.0)
R_{free}[b] (%)	29.1 (37.1)
No. of protein atoms	14,512
No. of other atoms[c]	162
Stereochemistry	
r.m.s.d. for bond lengths (Å)	0.023
r.m.s.d. for bond angles (°)	2.28
Residues in the Ramachandran plot	
Most favored region (%)	61.0
Additional allowed regions (%)	37.7
Generously allowed regions (%)	1.3

[a] $R_{cryst} = 100(\Sigma||F_o| - |F_c||/\Sigma|F_o|)$, where F_o and F_c are the structure factor amplitudes from the data and the model, respectively.
[b] R_{free} is R_{cryst} with 5% test set of structure factors.
[c] 84 atoms comprising 6 residues of *N*-acetyl-D-glucosamine and 78 atoms comprising 6 citrate ions.

which showed them to be virtually identical, demonstrating dimerization through highly specific interactions between the concave surfaces of the apposed LRR domains (27).

Here we show that biglycan forms stable dimers in solution and present the biglycan structure obtained by x-ray crystallography. Moreover, we provide strong evidence that dimerization is essential for the folding and structural stability of both decorin and biglycan.

EXPERIMENTAL PROCEDURES

Proteoglycans—Bovine skin decorin and bovine articular cartilage biglycan were isolated and purified as described (24, 28). The purified proteoglycans and their glycoprotein cores produced by digestion with chondroitin ABC lyase (EC 4.2.2.4, Seikagaku) or by chondroitin ABC lyase followed by *N*-glycosidase F (EC 3.2.2.18, Roche Applied Science) (12), were examined by gel electrophoresis in 12% polyacrylamide gels containing 0.1% (w/v) SDS, pH 8.6 (29). The protein cores of both proteoglycan preparations used here were sequenced in their entireties by Edman degradation (10, 30).

Crystallization of Biglycan—Biglycan was digested with chondroitin ABC lyase (EC 4.2.2.4, Seikagaku) at 37 °C for 3 h to remove the glycosaminoglycan chains (24). Guanidinium chloride (GdnHCl, 2.5 M) was added to the digestion mixture, and the core glycoprotein was then isolated by size-exclusion chromatography on a Superose 6™ HR10/30 column (Amersham Biosciences) eluted with 2.5 M GdnHCl in 0.02 M Tris-HCl/0.15 M NaCl, pH 7.0 (TBS). To the pooled fractions was added sodium azide, EDTA, and Zwittergent 3-14 (Calbiochem) to final concentrations of 0.02% (w/v), 5 mM and 0.01% (w/v), respectively. Protein was concentrated by ultrafiltration to 5.4 mg/ml, as measured by the BCA protein assay (31), and refolded by sequential dialysis against 0.5 M arginine/0.4 mM Zwittergent 3-14/TBS, pH 8.5 (16 h), 0.4 mM Zwittergent 3-14/TBS, pH 8.5 (8 h), and 0.4 mM Zwittergent 3-14/0.02% (w/v) NaN_3, pH 7.5 (16 h). Refolding was assessed by CD spectroscopy, and the solution molar mass of the protein was measured by size-exclusion chromatography/multiangle laser light scattering (24). Aliquots of refolded protein were diluted to 2.7 mg/ml in 0.4 mM Zwittergent 3-14/0.02% (w/v) NaN_3, pH 7.5. Crystals were grown by vapor diffusion in hanging drops consisting of 2 μl of protein solution and 2 μl of 0.2 M triammonium citrate/polyethylene glycol 3350 (20% v/v), pH 7.0, set up at 20 °C over 1 ml of the same solution. Triangular plate-like crystals, ~150 μm on edge and 15 μm thick, appearing after 2 months, were flash-cooled to 90 K in cryoprotectant consisting of 30% (w/v) D(−) glucose in well solution. Reflections were indexed in the space group C2 with unit cell dimensions $a = 206.511$ Å, $b = 110.222$ Å, $c = 140.625$ Å, $\alpha = 90°$, $\beta = 116.61°$, $\gamma = 90°$ and six biglycan monomers per asymmetric unit ($V_m = 3.45$ Å^3/Da, corresponding to a solvent content of 64.32%).

Data Collection and Processing—Data were collected at beamline 8.3.1 at the Advanced Light Source, Lawrence Berkeley National Laboratory, Berkeley, CA. The data were processed and scaled using the programs Mosflm, SCALA, and TRUNCATE, from the CCP4 program suite, run under the control of the Elves_1.2 automation scripts (32). Data collection statistics are summarized in Table 1.

Structure Solution and Refinement—The biglycan structure was solved by molecular replacement with Molrep7.4 (33) from the CCP4 suite, using the 2.15-Å crystal structure of the bovine decorin monomer (PDB code 1XKU) (27) as a probe ($R_{cryst} = 49.1\%$ and $R_{free} = 48.6\%$). The model was rebuilt into solvent-flattened electron density maps calculated using RESOLVE in "prime-and-switch" mode (34), and simulated annealing composite omit maps were calculated using the Crystallography and NMR System software package (CNS), version 1.1 (35). XFIT (36) was used to display maps and to build/rebuild models. Refinement to 3.4 Å was performed using simulated annealing in CNS to convergence ($R_{cryst} = 30.4\%$ and $R_{free} = 33.9\%$). Final refinement was carried out using REFMAC5.2 (37). Tight NCS restraints were applied during refinement in both CNS and REFMAC5. The final model ($R_{cryst} = 25.9\%$ and $R_{free} = 29.1\%$; Table 2) is composed of amino acid residues 25–327 of chains A, B, C and E, residues 25–328 of chain D, residues 25–329 of chain F, 6 *N*-acetyl-D-glucosamine residues, and 6 citrate anions. The refined coordinates have been deposited with the PDB and assigned the entry code 2FT3.

Circular Dichroism Spectroscopy—Samples of proteoglycan were dissolved in 0.15 M NaCl/0.02 M Tris-HCl, pH 7.0, with and without 2.5 M GdnHCl, at various protein concentrations. The actual concentrations were determined by the BCA assay. CD spectra were recorded between 190 and 250 nm on a Jasco J-720 spectropolarimeter. Denaturation curves were recorded by continuously monitoring the ellipticities at 205 nm or 217 nm in Jasco J-20 or J-720 spectropolarimeters. Thermostatted cells of 0.01-, 0.02-, 0.1-, and 1-cm path length were used for these experiments. Raw data were converted to mean residue ellipticities using mean residue weights of 110.3 for decorin and 112.2 for biglycan, respectively, calculated from their amino acid sequences. The kinetics of refolding of GdnHCl-denatured proteoglycans were followed by diluting aliquots of 2.5 M GdnHCl solutions into TBS and recording CD spectra at 2-min (for decorin) or 10-min (for biglycan) intervals, from 250 to 205 nm at a scan rate of 50 nm/min, starting 30 s after dilution.

Differential Scanning Calorimetry—Weighed samples of decorin were dissolved at ~1 mg/ml in 0.15 M NaCl/0.02 M Tris-HCl/0.02% (w/v) NaN_3, pH 7.0. Solutions were dialyzed overnight at 4 °C against 250 volumes of buffer, filtered through 0.45-μm membrane filters (Sartorius) and degassed for 10 min with stirring under vacuum. The actual concentra-

tions of protein in these solutions were determined by the BCA assay. A differential scanning microcalorimeter (VP-DSC, MicroCal Inc., Northampton, MA) was used in passive (*i.e.* no feedback) mode with a filter period of 16 s. Reference scans were performed first with both cells filled with sample dialysate. Following a pre-scan equilibration period of 15 min, the temperature was increased linearly from 25 to 60 °C at a rate of 0.5 °/min, followed by immediate cooling. Once a reproducible baseline had been obtained, the buffer in the sample cell was replaced with the solution of proteoglycan. The scan rate of 0.5 °/min was selected to give results for the T_m of decorin measured during an up-scan and the subsequent down-scan at the same rate, differing by <0.5 °C. To test for refolding of the denatured protein, up-scans were repeated with intermediate cooling at the default maximum rate (~5 °/min). Data were analyzed using MicroCal Origin™ software. Excess heat capacity curves obtained with buffer alone were subtracted from those obtained for decorin solutions.

Gel Chromatography and Light Scattering—Samples dissolved in TBS/0.02% (w/v) sodium azide were chromatographed on a Superose™ 6 HR 10/30 column eluted with the same buffer. The effluent from this column was led through multiangle laser light scattering (DAWN-F) and refractive index (Optilab 903) detectors (Wyatt Technologies, Santa Barbara, CA). ASTRA version 2 software was used to process data. A value for *dn*/*dc* of 0.14 was used for biglycan, calculated from the values of 0.15 and 0.12 previously determined for decorin and dermatan sulfate, respectively (38), taking into account the higher proportion of GAG in biglycan. To monitor the effect of temperature on the molecular weight, the buffer pump was stopped just after the material in the main decorin (dimer) peak had entered the light scattering and refractive index detectors, which were initially at 25 °C. The temperature was then increased at a rate of 2 °C/min, held at 60 °C for 5 min and then decreased at a rate of 2 °/min. After a further 8 min at 25 °C, buffer flow was resumed.

RESULTS

Fig. 1 shows a comparison by SDS-PAGE of the two proteoglycans and their core proteins. Intact biglycan migrates more slowly than decorin, but after removal of the GAG chains by digestion with chondroitin ABC lyase (*lanes 2* and *5*), its glycoprotein core migrates slightly faster than that of decorin. This behavior is consistent with the presence of two *N*-linked oligosaccharides on biglycan, compared with the three on decorin. The mobilities of the bands generated after further digestion with *N*-glycosidase F to remove these oligosaccharides (*lanes 3* and *6*) were indistinguishable. For crystallization of biglycan, as for decorin (27), only the GAG chains were removed, because we had found previously that removal of *N*-linked oligosaccharides leads to nonspecific aggregation and decreased solubility of the core protein of decorin (12).

The asymmetric unit of the biglycan crystal consists of six monomers organized as three antiparallel dimers, one of which is illustrated in Fig. 2. The dimer interface in biglycan buries a somewhat larger surface area than that in decorin (2550 Å^2 compared with 2300 Å^2). Similar to the structure that we recently solved for decorin (27), the biglycan monomer consists mainly of a right-handed spiral of 12 leucine-rich repeats, each of which comprises a short β-strand linked by loops, strands, and short helical segments (Fig. 2*A*). The β-sheet forming the inner concave face of the arch-shaped biglycan monomer begins with an anti-parallel hairpin stabilized by two disulfides. A third disulfide (between residues 285 and 318) connects LRRs 11 and 12 and stabilizes a loop that we have termed the "ear." The Cα atoms of the biglycan and decorin monomers can be superimposed with an average r.m.s.d. of 2.9 Å and the dimers (Fig. 2*B*) with an r.m.s.d. of 3.2 Å. The β-sheet face of the biglycan monomer is more tightly curved than in decorin.

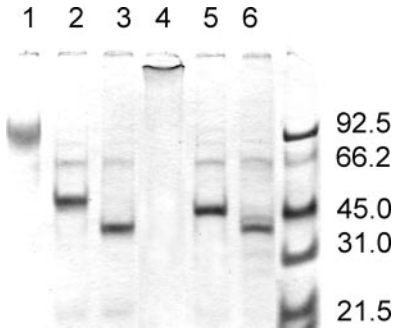

FIGURE 1. **Comparison by SDS-PAGE of decorin (*lanes 1–3*) and biglycan (*lanes 4–6*) with the intact proteoglycans (*lanes 1* and *4*), the core proteins produced from them by digestion with chondroitin ABC lyase (*lanes 2* and *5*), and by chondroitin ABC lyase followed by *N*-glycosidase F (*lanes 3* and *6*).** Each *lane* carries 10 μg of sample. Gels were stained with Coomassie Blue R250.

The near N-terminal cystine-knot arrangement of disulfides in biglycan, connecting Cys-27 to Cys-33 and Cys-31 to Cys-40 (Fig. 2*C*), is identical to that in decorin. This disagrees with an earlier conclusion that Cys-27 was connected to Cys-40, based on sequence analysis (30).

No electron density was observed for residues 1–24 or for residue 330 in any of the 6 molecules of biglycan in the asymmetric unit. These sequences were also unobserved in the crystal structure of decorin (27) and are assumed to be conformationally flexible.

At an early stage in the fitting of maps, strong electron density that could not be accounted for in terms of the known amino acid sequence, was observed near to the N terminus of each biglycan monomer. This density was contained within a pocket formed mainly by residues His-202, His-226, His-247, and Asp-249 of one protomer, partially closed off from solvent by residues Leu-43, Leu-45, and Lys-46 of the second protomer. It was initially thought that this electron density might be due to zinc, in view of reports that biglycan can bind this cation (39). However, potential electron donor atoms within the pocket are too far away from the putative metal ion for coordination. The position, discrete nature, and shape of this electron density are also inconsistent with a covalently attached sugar residue. A single citrate ion, most probably derived from the crystallization solution, was eventually fitted at each location (Fig. 2*D*).

Comparison between native and GdnHCl (2.5 M) denatured decorin and biglycan (Fig. 3) shows that denaturation results in complete abolition of the negative Cotton effect near 217 nm. Changes in CD reflect alterations only in the secondary structures of the protein cores, because the GAG chains and *N*-linked oligosaccharides contribute little to the spectra (23).

Panels A and *B* in Fig. 4 show denaturation curves measured for the two proteoglycans by monitoring the ellipticity at 217 nm as a function of the concentration of GdnHCl. From plots of Δ*G versus* concentration of denaturant over the approximately linear portions of the curves (*panels C* and *D*) (40), the net stabilities at 25 °C in the absence of denaturant are estimated to be −1.57 ± 0.04 and −1.92 ± 0.16 kcal.mol^{-1}, for decorin and biglycan, respectively. The concentrations of GdnHCl giving 50% denaturation are 0.753 ± 0.008 and 0.954 ± 0.154 M, and the slopes are 2.081 ± 0.033 and 1.693 ± 0.146 kcal.mol^{-1}.M^{-1}, respectively. Samples of decorin and biglycan that had been dissolved in 2.5 M GdnHCl and then dialyzed against buffer overnight at 4 °C gave CD spectra that were indistinguishable from those shown in Fig. 3 for the native proteoglycans. Denaturation by GdnHCl is therefore completely reversible.

Circular dichroism spectroscopy was used to investigate the kinetics of refolding following dilution of 2.5 M GdnHCl solutions into TBS. At a concentration of 2.92 μM denatured decorin (Fig. 5*A*) refolded com-

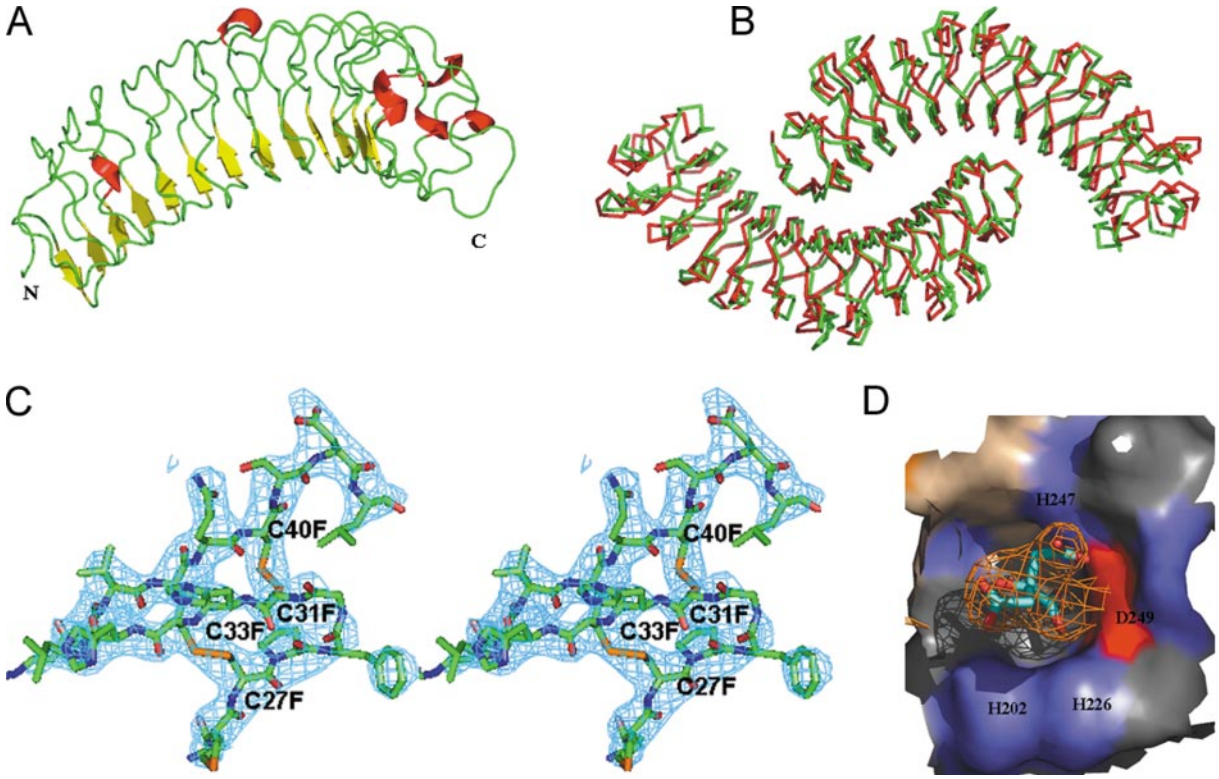

FIGURE 2. *A*, schematic representation of the structure of the biglycan monomer. Strands are colored *yellow*, helices *red*, and other secondary structures *green*. *B*, overlay of C-α atoms of biglycan (*green*) and decorin (*red*) dimers. Structures were overlaid in Xfit (McRee (36)). *C*, wall-eyed stereo view of calculated electron density ($2mF_o - DF_c$, contoured at 1.5 σ) around the near N-terminal disulfide knot in biglycan, showing cysteine residues 27 linked to 33 and 31 linked to 40. *D*, calculated electron density ($2mF_o - DF_c$, contoured at 1.5 σ) around citrate ion, together with the surfaces of nearby residues. Electron densities were calculated using CNS version 1.1 (Brünger *et al.* (35)). All figures were generated using PYMOL version 0.97 (pymol.sourceforge.net/).

pletely within 2 min. At higher dilution (0.77 μM), refolding was slower. Biglycan (Fig. 5*B*) refolded more slowly than decorin: at a concentration of 2.57 μM, refolding appeared to be complete by ~40 min. As seen for decorin, refolding of biglycan was slower at lower concentrations. Proteoglycans at concentrations intermediate between those shown refolded at intermediate rates (data not shown). Therefore, the rate of refolding of both the decorin and biglycan was concentration-dependent.

Light scattering was used to measure the molecular weights of the proteoglycans in TBS initially and after refolding in CD experiments. We have previously published light scattering data for decorin in TBS, in 2.5 M GdnHCl and following dilution from 2.5 M GdnHCl back into TBS during chromatography (24). As seen for decorin, in 2.5 M GdnHCl (Fig. 6*A*) biglycan was monomeric with molar mass of ~60 kDa, but following dilution into TBS it was recovered as dimer (125.8 ± 13.0 kDa, mean ± 1 S.D., 5 independent experiments), even when it had been diluted to concentrations as low as 0.77 μM.

Thermal denaturation is characterized in the spectropolarimeter by a decrease in ellipticity at wavelengths below 215 nm (Fig. 7). The denaturation curve for decorin (Fig. 7*B*) shows a single cooperative transition with a mid-point (T_m) near 46 °C. A similarly progressive decrease in ellipticity at 205 nm was seen for biglycan at temperatures above 37 °C, but there was a marked discontinuity in the denaturation curve (Fig. 7*D*) at ~50 °C. Consequently, a sigmoid curve could not be fitted to these data, and T_m could not be estimated. Solutions of biglycan recovered from the CD cell after thermal denaturation were found by light scattering to contain mainly high molecular weight aggregate. The CD spectrum of biglycan at 60 °C is markedly different from that of decorin, showing a single minimum at ~208 nm. After cooling to 25 °C, heat-denatured decorin completely recovered its secondary structure (Fig. 7*A*), but biglycan did not, as evidenced by the broad minimum centered

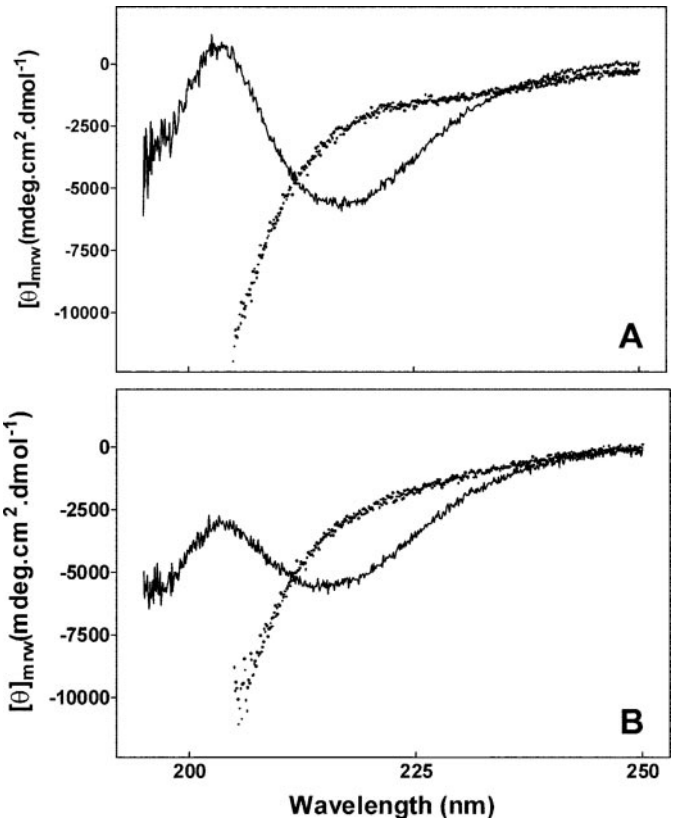

FIGURE 3. **CD spectra for decorin (*A*) and biglycan (*B*).** Spectra recorded in 0.02 M Tris/0.15 M NaCl, pH 7.0, at 25 °C in the absence (*continuous line*) and presence (*dotted line*) of 2.5 M GdnHCl.

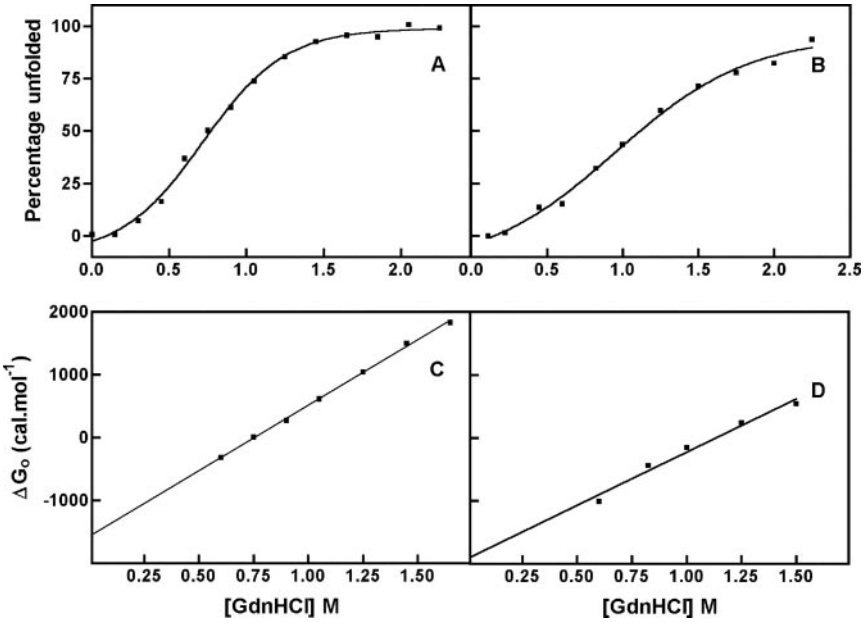

FIGURE 4. Denaturation of decorin (*A*) and biglycan (*B*) by GdnHCl. Ellipticities at 217 nm were recorded over 5 min at a sampling rate of 1 Hz, and the data were averaged. Percentage unfolded was calculated assuming that the protein was completely native at 0 M GdnHCl and completely unfolded at 2.5 M. *C* and *D*, plots of Δ*G versus* denaturant concentration for the data in *A* and *B*, respectively.

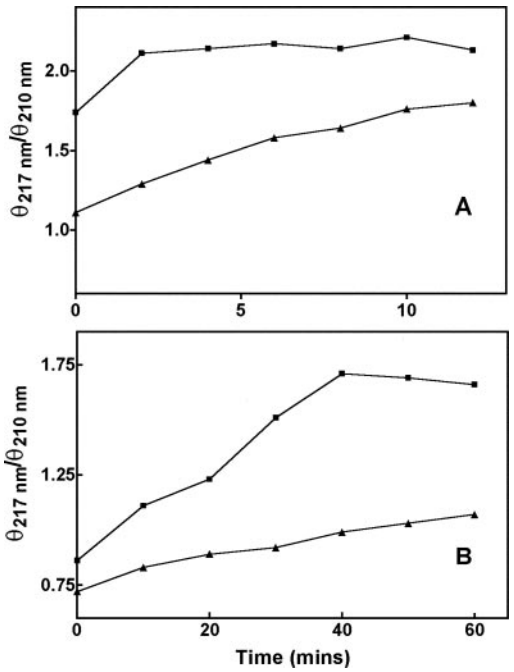

FIGURE 5. **Refolding of GdnHCl-denatured decorin (*A*) and biglycan (*B*), monitored by CD.** Protein concentrations (expressed as monomer) were 2.92 μM (*squares*) and 0.77 μM (*triangles*) for decorin and 2.57 μM (*squares*) and 0.83 μM (*triangles*) for biglycan.

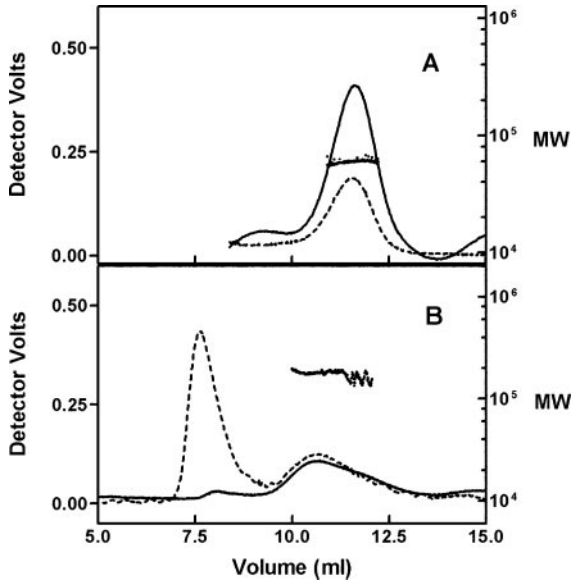

FIGURE 6. **Gel chromatography of biglycan with molecular weight determination by multi-angle laser light scattering.** *A*, biglycan dissolved in 2.5 M GdnHCl/TBS and chromatographed in the same buffer. *B*, biglycan recovered after 20-fold dilution from 2.5 M GdnHCl into TBS. The *solid line* shows the refractive index detector signal, and the *broken line* shows light scattering intensity. The superimposed (*dotted*) plots show the molecular weights as a function of elution volume.

around 215 nm (compare the 25 °C profile in Fig. 7*C* with that in Fig. 3*B* for native biglycan).

The complete recovery of the secondary structure of decorin following heat denaturation under the conditions used here allowed further thermal denaturation studies to be undertaken. Differential scanning calorimetry of decorin confirmed a single thermal transition with a mid-point close to that measured by CD (Fig. 8*A*). As shown in Fig. 8*B*, these calorimetric data closely fit a "two-state" model of the denaturation process only when the protein concentration was calculated assuming the decorin is dimeric rather than monomeric at the onset of denaturation. The enthalpy of denaturation estimated from these four superimposable curves is 123.3 ± 1.3 kcal.mol^{-1} (mean ± 1 S.D.), and the T_m is 45.4 ± 0.1 °C. Circular dichroism spectroscopy confirmed that the decorin regained all its secondary structure on cooling to 25 °C after thermal denaturation in the calorimeter (the spectrum was indistinguishable from that shown in Fig. 3), and light scattering showed this refolded decorin to be dimeric.

The presence of the reducing agent Tris(2-carboxyethyl)phosphine HCl abolished all refolding of decorin in the calorimeter after the initial up-scan (Fig. 8*C*). A further three scans in the presence of Tris(2-carboxyethyl)phosphine HCl (not shown) showed no subsequent recovery. The T_m and enthalpy of denaturation (46.6 °C and 145.4 kcal.mol^{-1}) measured during the initial up-scan in the presence of reducing agent were, within experimental error, the same as in its absence, showing that reduction of disulfides occurs only after denaturation.

Finally, we investigated the effect of denaturation on the molar mass of decorin by monitoring light scattering intensity as a function of tempera-

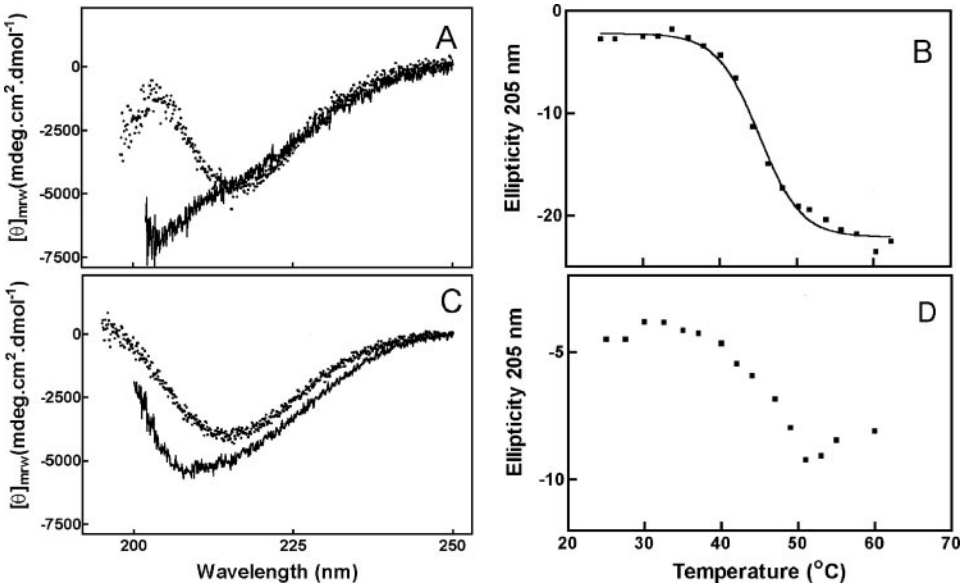

FIGURE 7. **Thermal denaturation of decorin and biglycan monitored by circular dichroism.** Spectra recorded at 60 °C (*solid lines*) for decorin (*A*) and biglycan (*C*), and after subsequent cooling to 25 °C (*dotted lines*). *Panels B* and *D* show denaturation curves for decorin and biglycan, respectively. The *solid line* in *panel B* shows the fit of a sigmoid curve to the data for decorin.

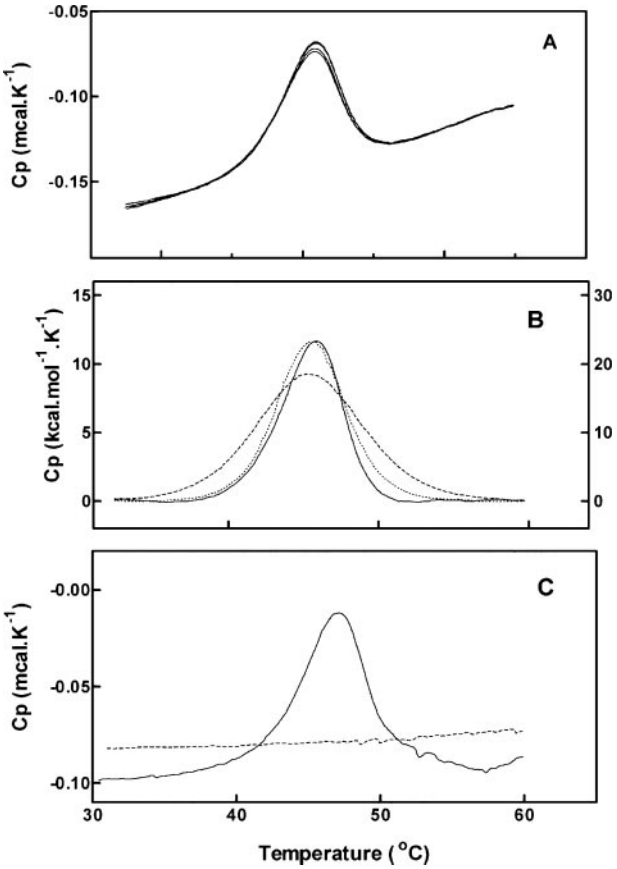

FIGURE 8. **Thermal denaturation of decorin studied by microcalorimetry.** The sample concentration (expressed as dimer) was 11.7 μM. Four successive up-scans are shown superimposed in *panel A*. *B*, fit of calculated to experimental data assuming that the cooperative unfolding unit is either a monomer (*dashed line*) or a dimer (*dotted line*). To prepare the raw data for fitting, a flat baseline was drawn under the curves in *panel A*, thus treating ΔC_p as zero. *C*, effect of reduction of disulfides on the reversibility of thermal denaturation of decorin, as assessed by microcalorimetry: the first (*solid line*) and second (*dashed line*) up-scans are shown for decorin (11.7 μM) in the presence of 100 μM Tris(2-carboxyethyl)phosphine HCl.

ture. As shown in Fig. 9, heating a solution of decorin to a temperature above the T_m was accompanied by a reduction in light-scattering intensity and a 2-fold reduction in molar mass (*i.e.* a transition from dimer to monomer). On cooling, there was an immediate and sharp increase in light-scattering intensity accompanying the reformation of the dimer. This experiment was repeated three times with the same result.

DISCUSSION

Here we show that biglycan, like decorin, is dimeric in solution and crystallizes as a dimer. This is in agreement with a previously published ultracentrifugation study that demonstrated dimerization of biglycan (39). The biglycan dimer closely resembles that of decorin, and there is high conservation of residues at the interface. These residues are also conserved in asporin, the third Class I SLRP, strongly suggesting that all three dimerize in the same way. However, the biglycan dimer does have some unique features, including a histidine-lined pocket that is likely to provide a binding site for a complex anion. Alignment of the sequences of the three Class I SLRPs (decorin, biglycan, and asporin), with the residues that become buried as a consequence of dimerization *boxed*, is shown in Fig. 10. The degree of conservation of these residues (72% identical and an additional 17% similar) is much greater than that for the protein cores as a whole (42% identical and an additional 33% similar). One notable difference is the replacement of Arg-28 in decorin by Gly in both biglycan and asporin. In decorin, this Arg residue adopts a rather unusual strained α_L conformation and forms a salt bridge with Asp-200 of the other protomer. The lack of this particular interaction might account in part for the slower refolding of biglycan. It would be of considerable interest to carry out the physical studies described here for decorin and biglycan, on asporin when that protein becomes available in sufficient amounts.

The solution x-ray scattering data obtained for decorin (24) show that the flexible N-terminal segments of the protein core direct the GAG chains away from it so that they mix with solvent. Because we saw no electron density that could be assigned to the GAG chain stubs left by the action of chondroitin ABC-lyase, in either decorin or biglycan, we assume that these do not interact with the protein cores or contribute to the stabilities of the dimers.

Decorin and biglycan are both very easily denatured, as reflected in the low concentrations of GdnHCl required and in the low T_m (45–46 °C). The net stabilities estimated from the denaturation curves for the two samples studied here (~ -1.6 and -1.9 kcal.mol^{-1}) are quite similar and both values are much lower than those for many globular proteins (41). We do not yet know whether this low stability has any

physiological significance, but it could obviously affect the interpretation of functional studies such as those using mutagenesis to probe the determinants of biological activity. Conclusions from such studies on decorin and biglycan should be treated with caution unless supported by evidence for unaltered three-dimensional structure and stability of the mutant proteins.

We found that biglycan underwent irreversible self-aggregation on heat denaturation, whereas the heat denaturation of decorin was completely reversible. Nevertheless, the initial thermal stability of biglycan seems to be comparable to that of decorin, as changes in the CD spectra become apparent at the same temperature (*i.e.* just above 37 °C). Interestingly, the CD spectra of biglycan and decorin at 60 °C differ: that for decorin is essentially featureless above 200 nm, whereas the negative peak near 208 nm observed for biglycan might indicate retention of some secondary structure, possibly stabilized by self-aggregation. Reversible heat denaturation of decorin was confirmed in several independent experiments using both differential scanning calorimetry and CD spectroscopy. The unchanging values for T_m and enthalpy, measured from four successive up-scans in the calorimeter, show that the same species is involved in the transition each time. This was confirmed by CD spectroscopy, which showed that the secondary structure of decorin recovered from the calorimeter after cooling was identical to that of the starting material. This reversible denaturation of decorin allowed us to undertake additional experiments that were not possible with biglycan.

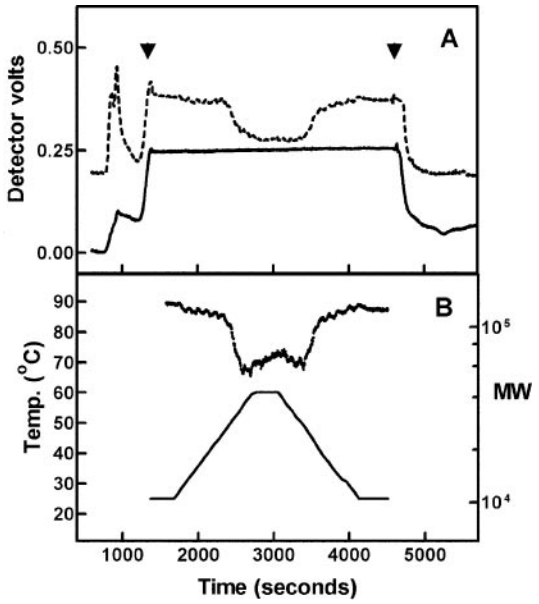

FIGURE 9. **Molecular weight of decorin monitored as a function of temperature by stopped-flow chromatography and multiangle laser light scattering.** *A*, refractive index (*solid line*) and light-scattering (*broken line*) detector signals. *B*, temperature (*solid line*) and molecular weight (*upper plot*). *Arrowheads* indicate the times at which buffer flow was stopped and restarted. The strong light scattering peak at V_o is due to the presence of a small amount of particulate material or high molecular weight aggregate. Its separation from the main dimer peak ensures that it does not interfere with the molecular weight determination of the latter (24).

The reversibility of the denaturation of decorin reported here is in marked contrast to the reported behavior of a sample of recombinant decorin produced in a vaccinia virus/T7 bacteriophage expression system (42). Those investigators found that their urea-denatured recombinant decorin did not recover secondary structure on dialysis against urea-free buffer, whereas here we demonstrate complete recovery after exposure to GdnHCl. Neither did their decorin recover after heating to 60 °C, whereas here we demonstrate complete refolding after four (or more) cycles of heating and cooling. It is possible that the lack of one or more disulfides is responsible for the reported inability of their decorin to refold, as we have shown here that disulfide bonding is of critical importance in this process. Indeed we suggest that the ability of samples to refold completely after denaturation in chaotropes represents a good quality control for decorin and biglycan.

Three different sets of experiments provide strong evidence that dimerization is essential for the structural stability of decorin and biglycan; indeed, in all our experiments we never found any evidence for the existence of folded monomers. Firstly, the rate of refolding of decorin and biglycan after denaturation in 2.5 M GdnHCl was concentration-dependent, with both refolding more slowly in more dilute solutions. This

```
Dcn -DEASGIGPEEHFPEVPEIEP-MGPVCPFRCQCHLRVVQCSDLGLEKVPKDLPPDTALLD
Bgn DEEASGAETTSGIPDLDSLPPTYSAMCPFGCHCHLRVVQCSDLGLKAVPKEISPDTTLLD
Asn DEDNSLFPTRE--PRSHFFPFDLFPMCPFGCQCYSRVVHCSDLGLTSVPTNIPFDTRMLD
     :: *   . .  *    :      .:*** *:*: ***:*****  **.::. ** :**

    LQNNKITEIKDGDFKNLKNLHTLILINNKISKISPGAFAPLVKLERLYLSKNQLKELPEK
    LQNNDISELRKDDFKGLQHLYALVLVNNKISKIHEKAFSPLRKLQKLYISKNHLCEIPPN
    LQNNKIKEIKENDFKGLTSLYGLILNNNKLTKIHPKAFLTTKKLRRLYLSHNQLSEIPLN
    ****.*.*::..***.*  *: *:* ***::**   ** .  **.:**.*.*:* *:* :

    MPKTLQELRVHENEITKVRKSVFNGLNQMIVVELGTNPLKSSGIENGAFQGMKKLSYIRI
    LPSSLVELRIHDNRIRKVPKGVFSGLRNMNCIEMGGNPLENSGFEPGAFDGLK-LNYLRI
    LPKSLAELRIHENKVKKIQKDTFKGMNALHVLEMSANPLDNNGIEPGAFEGVT-VFHIRI
    :*.:* ***.*:*.: *: *..*.*:. : :*:. ***...*:* ***:*:. : ::**

    ADTNITTIPQGLPPSLTELHLDGNKITKVDAASLKGLNNLAKLGLSFNSISAVDNGSLAN
    SEAKLTGIPKDLPETLNELHLDHNKIQAIELEDLLRYSKLYRLGLGHNQIRMIENGSLSF
    AEAKLTSVPKGLPPTLLELHLDYNKISTVELEDFKRYKELQRLGLGNNKITDIENGSLAN
    :::::* :*:.** :* ***** ***  ::  .:   .:* :*** *.*  ::****:

    TPHLRELHLNNNKLVKVPGGLADHKYIQVVYLHNNNISAIGSNDFCPPGYNTKKASYSGV
    LPTLRELHLDNNKLSRVPAGLPDLKLLQVVYLHTNNITKVGVNDFCPVGFGVKRAYYNGI
    IPRVREIHLENNKLKKIPSGLPELKYLQIIFLHSNSIARVGVNDFCPTVPKMKKSLYSAI
     * :**:**:**** ::*.**.: * :*:::**.*.*: :* *****     *:: *..:

    SLFSNPVQYWEIQPSTFRCVYVRAAVQLGNY--
    SLFNNPVPYWEVQPATFACVTDRLAIQFGNYKK
    SLFNNPVKYWEMQPATFRCVLSRMSVQLGNFGM
    ***.*** ***:**:** **  * ::*:**:
```

FIGURE 10. **Alignment of the amino acid sequences of bovine decorin (*Dcn*), bovine biglycan (*Bgn*), and human asporin (*Asn*).** Residues that are known (in decorin and biglycan) or postulated (in asporin) to become buried as a consequence of dimerization, are shown in *boxes*.

shows that renaturation cannot be a purely unimolecular process. Secondly, the good fit of a two-state model to the calorimetry data strongly suggests that the cooperative unfolding unit is a dimer and that denaturation and dissociation are inseparable processes, as are refolding and dimerization. Thirdly, compelling data were obtained by measuring light scattering during the thermal denaturation and renaturation of decorin. This showed that the molecular weight of the decorin halved (*i.e.* there was a dimer to monomer transition) exactly coinciding with thermal denaturation, and transition from monomer to dimer exactly coincided with renaturation during cooling. Therefore, the folding is dependent upon dimerization and, given the low net stabilities of the dimers of decorin and biglycan, it is unlikely that either protein core could exist in a folded state at 37 °C without the stabilization energy conferred by dimerization. Although this dependence on dimerization for stability may be unusual, it is by no means unknown, interleukin-10 being one other example of a protein that may not exist as a folded monomer (43).

Goldoni *et al.* (26) claimed that "biologically active" decorin is a monomer in solution. However, our data show that decorin and biglycan must be dimeric to be in a folded state, implying that their decorin was either unfolded (and its reported biological activity not dependent upon the folding) or that it was in fact dimeric. Both are possibilities, because no data were presented on the secondary structure of the decorin of Goldoni *et al.*, and the techniques used to determine oligomerization state (chemical cross-linking, MALDI-TOF mass spectrometry, and gel-filtration chromatography using globular protein standards) are not as robust as the biophysical and structural techniques used here and in our previous work (24, 25, 27). Those authors found that relatively high concentrations of cross-linking agents were required to cross-link decorin compared with other known dimers, such as the epidermal growth factor receptor, and concluded that the decorin was monomeric. However, the ability to cross-link depends far more on the availability of appropriately spaced lysine residues than on the concentration of cross-linker and inspection of the crystal structure of the decorin dimer (PDB code 1XEC) shows that only 2 of 54 lysine residues approach close enough to possibly cross-link the dimer. Therefore this argument is weak. Mass spectrometry gives data about oligomerization state *in vacuo*, not in solution. Moreover, samples for MALDI-TOF mass spectrometry experiments were prepared in 10 mg/ml sinapinic acid in 30% (v/v) acetonitrile. Decorin is denatured at low pH[5] and will therefore be monomeric under these conditions. The third line of evidence came from gel-filtration experiments where it was shown that the K_{av} for decorin core protein on a Superose 6 column is 0.62, and, by comparison with globular protein standards, it was concluded that the molecular mass (~55 kDa) was consistent with a monomer. We obtained the identical K_{av} for decorin core protein on a Superose 6 column but showed by light scattering that this corresponds to a mass of 84.6 ± 4 kDa, *i.e.* it is unequivocally a dimer (24).

One limitation of the present work is that here we have studied only pure decorin and biglycan in solution. While seeming unlikely on energetic grounds, it is theoretically possible that these dimers dissociate (and possibly unfold), on binding to other extracellular matrix macromolecules. Nevertheless, the structures we have determined have important implications for understanding how these macromolecules interact with their biological ligands, as discussed elsewhere (45).

In conclusion, we have demonstrated that biglycan forms stable dimers in solution and crystallizes as dimers. Furthermore, we could not find any evidence that folded decorin or biglycan exist as monomers in solution. The requirement of dimerization for native folding and stability suggests a novel role for the parallel β-sheet face of these and possibly other SLRPs and LRR proteins, namely self-recognition and structure stabilization. The elucidation of the structures of these SLRPs gives new impetus to studies on their ligand binding and dimerization and provides a possible explanation for their affinity toward a variety of dimeric ligands such as the transforming growth factor-β and the epidermal growth factor receptor (7, 44).

Acknowledgments—We thank Sophie Lehocky and Leigh Ann Giebelhaus for technical assistance. We thank Dr. Cyril M. Kay for critical reading of the manuscript.

[5] P. G. Scott, unpublished data.

REFERENCES

1. Henry, S. P., Takanosu, M., Boyd, T. C., Mayne, P. M., Eberspaecher, H., Zhou, W., de Crombrugghe, B., Hook, M., and Mayne, R. (2001) *J. Biol. Chem.* **276,** 12212–12221
2. Scott, J. E. (1993) in *Dermatan Sulphate and Dermatan Sulphate Proteoglycans: Chemistry, Biology, Chemical Pathology* (Scott, J. E., ed) pp. 165–181, Portland Press, London
3. Danielson, K. G., Baribault, H., Holmes, D. F., Graham, H., Kadler, K. E., and Iozzo, R. V. (1997) *J. Cell Biol.* **136,** 729–743
4. Scott, J. E., and Haigh, M. (1985) *Biosci. Rep.* **5,** 71–81
5. Yamaguchi, Y., Mann, D. M., and Ruoslahti, E. (1990) *Nature* **346,** 281–284
6. Hakkinen, L., Strassburger, S., Kahari, V. M., Scott, P. G., Eichstetter, I., Iozzo, R., and Larjava, H. (2000) *Lab. Invest.* **80,** 1869–1880
7. Zhu, J.-X., Goldoni, S., Bix, G., Owens, R. T., McQuillan, D. J., Reed, C. C., and Iozzo, R. W. (2005) *J. Biol. Chem.* **280,** 32468–32479
8. Krusius, T., and Ruoslahti, E. (1986) *Proc. Natl. Acad. Sci. U. S. A.* **83,** 7683–7687
9. Day, A. A., McQuillan, C. I., Termine, J. D., and Young, M. R. (1987) *Biochem. J.* **248,** 801–805
10. Scott, P. G. (1993) in *Dermatan Sulphate and Dermatan Sulphate Proteoglycans: Chemistry, Biology, Chemical Pathology* (Scott, J. E., ed) pp. 81–101, Portland Press, London
11. Chopra, R. K., Pearson, C. H., Pringle, G. A., Fackre, D. S., and Scott, P. G. (1985) *Biochem. J.* **232,** 277–279
12. Scott, P. G., and Dodd, C. M. (1990) *Connect. Tissue Res.* **24,** 225–236
13. Fisher, L. W., Termine, J. D., and Young, M. F. (1989) *J. Biol. Chem.* **264,** 4571–4576
14. Fisher, L. W., Termine, J. D., Dejter, S. W., Shitson, S. W., Yanagashita, M., Kimura, J. H., Hascall, V. C., Kleinman, H. K., Hassel, J. R., and Nilsson, B. (1983) *J. Biol. Chem.* **258,** 6588–6594
15. Rosenberg, L. C., Choi, H. U., Tang, L. H., Johnson, T. L., Pal, S., Webber, C., Reiner, A., and Poole, A. R. (1985) *J. Biol. Chem.* **260,** 6304–6313
16. Scott, P. G., Nakano, T., and Dodd, C. M. (1997) *Biochim. Biophys. Acta* **1336,** 254–262
17. Xu, T., Bianco, P., Fisher, L. W., Longenecker, G., Smith, E., Goldstein, S., Bonadio, J., Boskey, A., Heegaard, A. M., Sommer, B., Satomura, K., Dominguez, P., Zhao, C., Kulkarni, A. B., Robey, P. G., and Young, M. F. (1998) *Nat. Genet.* **20,** 78–82
18. Bianco, P., Fisher, L. W., Young, M. F., Termine, J. D., and Robey, P. G. (1990) *J. Histochem. Cytochem.* **38,** 1549–1563
19. Brown, D. C., and Vogel, K. G. (1989) *Matrix* **9,** 468–478
20. Schonherr, E., Witsch-Prehm, P., Harrach, B., Robenek, H., Rauterberg, J., and Kresse, H. (1995) *J. Biol. Chem.* **270,** 2776–2783
21. Matsushima, N., Ohyanagi, T., Tanaka, T., and Kretsinger, R. H. (2000) *Proteins Struct. Funct. Genet.* **38,** 210–225
22. Kobe, B., and Deisenhofer, J. (1994) *Trends Biochem. Sci.* **19,** 415–421
23. Scott, P. G., Winterbottom, N., Dodd, C. M., Edwards, E., and Pearson, C. H. (1986) *Biochem. Biophys. Res. Commun.* **138,** 1348–1354
24. Scott, P. G., Grossmann, J. G., Dodd, C. M., Sheehan, J. K., and Bishop, P. N. (2003) *J. Biol. Chem.* **278,** 18353–18359
25. Le Goff, M. M., Hindson, V. J., Jowitt, T. A., Scott, P. G., and Bishop, P. N. (2003) *J. Biol. Chem.* **278,** 45280–45287
26. Goldoni, S., Owens, R. T., McQuillan, D. J., Shriver, Z., Sasisekharan, R., Dirk, D. E., Campbell, S., and Iozzo, R. V. (2004) *J. Biol. Chem.* **279,** 6606–6612
27. Scott, P. G., McEwan, P. A., Dodd, C. M., Bergmann, E. M., Bishop, P. N., and Bella, J. (2004) *Proc. Natl. Acad. Sci. U. S. A.* **101,** 15633–15638
28. Choi, H. U., Johnson, T. L., Pal, S., Tang, L.-H., Rosenberg, L., and Neame, P. J. (1989) *J. Biol. Chem.* **264,** 2876–2884
29. Mechanic, G. (1979) in *Skeletal Research: An Experimental Approach.* (Simmons, D. J., and Kumin, S., eds) pp. 227–241, Academic Press, New York
30. Neame, P. J., Choi, H. U., and Rosenberg, L. C. (1989) *J. Biol. Chem.* **264,** 8653–8661
31. Smith, P. K., Krohn, R. I., Hermanson, G. T., Mallia, A. K., Gartner, F. H., Provenzano,

M. D., Fujimoto, E. K., Goeke, N. M., Olson, B. J., and Klenk, D. C. (1985) *Analyt. Biochem.* **150,** 76–85
32. Holton, J., and Alber, T. (2004) *Proc. Natl. Acad. Sci. U. S. A.* **101,** 1537–1542
33. Vagin, A., and Teplyakov, A. (1997) *Acta Crystallogr. Sect. D* **30,** 1022–1025
34. Terwilliger, T. C. (2001) *Acta Crystallogr. Sect. D* **57,** 1763–1775
35. Brünger, A. T., Adams, P. D., Clore, G. M., DeLano, W. L., Gros, P., Grosse-Kuntsleve, R. W., Jiang, J. S., Kuszewski, J., Nilges, M., Pannu, N. S., Read, R. J., Rice, L. M., Simonson, T., and Warren, G. L. (1998) *Acta Crystallog. sect D* **54,** 905–921
36. McRee, D. E. (1999) *J. Struct. Biol.* **125,** 156–165
37. Murshudov, G. N., Vagin, A., and Dodson, E. J. (1997) *Acta Crystallogr. Sect. D* **53,** 240–255
38. Zangrando, D. W., Gupta, R., Jamieson, A. M., Blackwell, J., and Scott, P. G. (1989) *Biopolymers* **28,** 1295–1308
39. Liu, J., Laue, T. M., Choi, H. U., Tang, L.-H., and Rosenberg, L. C. (1994) *J. Biol. Chem.* **269,** 28366–28373
40. Pace, C. N. (1986) *Methods Enzymol.* **131,** 266–280
41. Makhatadze, G. I., and Privalov, P. L. (1995) *Adv. Prot. Chem.* **47,** 307–425
42. Krishnan, P., Hocking, A. M., Scholtz, J. M., Pace, C. N., Holik, K. K., and McQuillan, D. J. (1999) *J. Biol. Chem.* **274,** 10945–10950
43. Zdanov, A., Schalk-Hihi, C., Gustchina, A., Tsang, M., Weatherbee, J., and Wlodawer, A. (1995) *Structure* **3,** 591–601
44. Hildebrand, A., Romaris, M., Rasmussen, L. M., Heinegard, D., Twardzik, D. R., Border, W. A., and Ruoslahti, E. (1994) *Biochem. J.* **302,** 527–534
45. McEwan, P. A., Scott, P. G., Bishop, P. N., and Bella, J. (2006) *J. Struct. Biol.*, in press